3-20-2023

Adiponectin-Mediated Promotion of CD44 Suppresses Diabetic Vascular Inflammatory Effects

Yanru Duan

Shihan Zhang

Yuanyuan Xing

Ye Wu

Wen Zhao

See next page for additional authors

iScience

CellPress
OPEN ACCESS

Article

Adiponectin-mediated promotion of CD44 suppresses diabetic vascular inflammatory effects

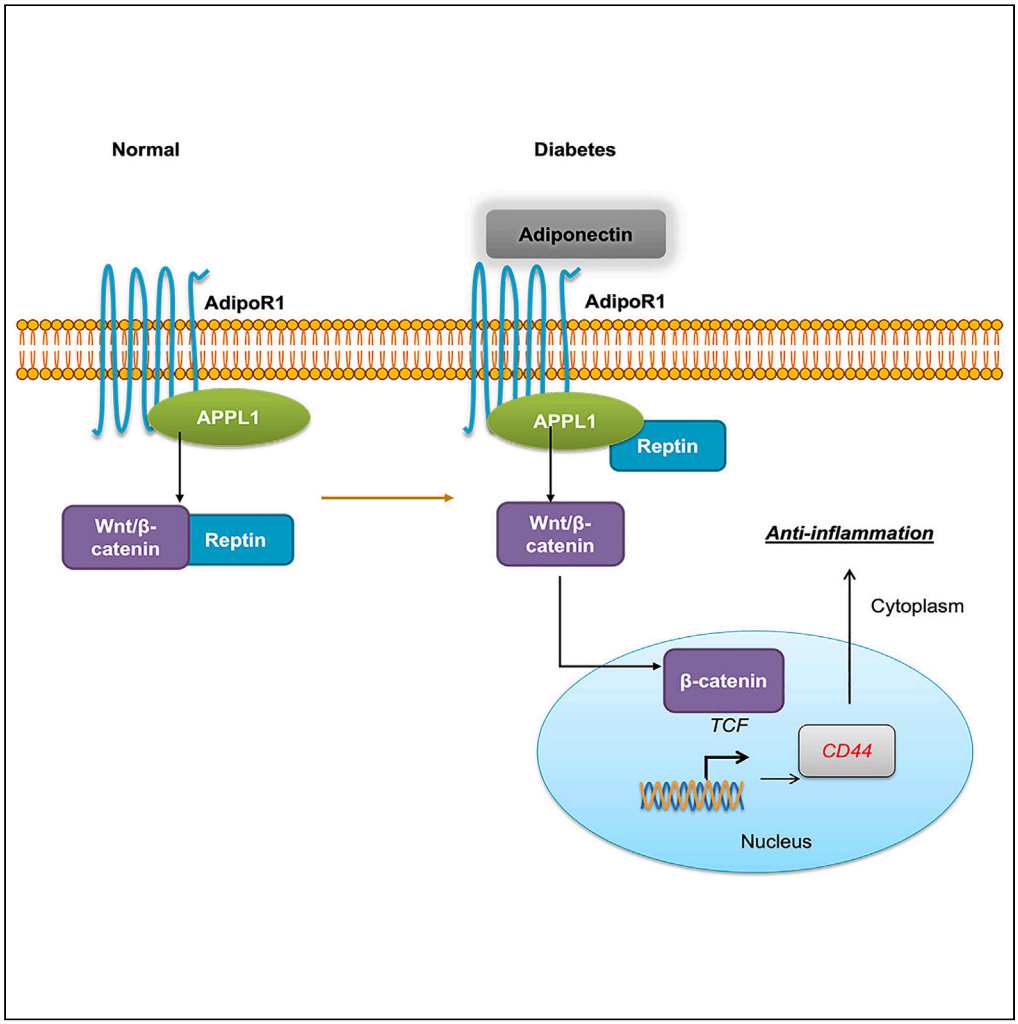

Yanru Duan, Shihan Zhang, Yuanyuan Xing, ..., Xinliang Ma, Yunhui Du, Huirong Liu

annahhdu820@mail.ccmu.edu.cn (Y.D.)
liuhr2000@ccmu.edu.cn (H.L.)

Highlights

APN inhibited vascular inflammation via the APPL1/Wnt/β-catenin/CD44 signaling axis

APN-mediated promotion of CD44 as a new mechanism suppresses vascular inflammation

CD44 represents a therapeutic target against vascular inflammation in diabetes

Duan et al., iScience 26, 106428
April 21, 2023
https://doi.org/10.1016/j.isci.2023.106428

iScience

CellPress
OPEN ACCESS

Article

Adiponectin-mediated promotion of CD44 suppresses diabetic vascular inflammatory effects

Yanru Duan,[1] Shihan Zhang,[2] Yuanyuan Xing,[3] Ye Wu,[1,4] Wen Zhao,[5] Pinxue Xie,[6] Huina Zhang,[5] Xinxiao Gao,[6] Yanwen Qin,[5] Yajing Wang,[7] Xinliang Ma,[7] Yunhui Du,[5,8,*] and Huirong Liu[1,4,*]

SUMMARY

While adiponectin (APN) was known to significantly abolish the diabetic endothelial inflammatory response, the specific mechanisms have yet to be elucidated. Aortic vascular tissues from mice fed normal and high-fat diets (HFD) were analyzed by transcriptome analysis. GO functional annotation showed that APN inhibited vascular endothelial inflammation in an APPL1-dependent manner. We confirmed that activation of the Wnt/β-catenin signaling plays a key role in APN-mediated anti-inflammation. Mechanistically, APN promoted APPL1/reptin complex formation and β-catenin nuclear translocation. Simultaneously, we identified APN promoted the expression of CD44 by activating TCF/LEF in an APPL1-mediated manner. Clinically, the serum levels of APN and CD44 were decreased in diabetes; the levels of these two proteins were positively correlated. Functionally, treatment with CD44 C-terminal polypeptides protected diabetes-induced vascular endothelial inflammation *in vivo*. Collectively, we provided a roadmap for APN-inhibited vascular inflammatory effects and CD44 might represent potential targets against the diabetic endothelial inflammatory effect.

INTRODUCTION

Type 2 diabetes mellitus (T2DM) and associated complications are a major public health concern worldwide.[1] Increased fatty acid oxidation and decreased glucose metabolism contribute to the development of diabetes.[2] Type 2 diabetes is characterized by a high glucose and high lipid (HG/HL) state.[3] A previous report exhibited that HG/HL significantly induces an endothelial inflammatory response, which contributes to vascular injury.[4] However, underlying mechanisms remain incompletely understood.

Adiponectin (APN) is an adipocyte-derived protein with anti-inflammatory, anti-diabetic, and anti-atherogenic effects.[5] Extensive clinical studies have shown that plasma APN, particularly the high molecular weight form, is reduced in patients with diabetes.[6] Hypoadiponectinema is an independent diabetic risk factor. Adiponectin knockout ($APN^{-/-}$) mice manifest increased inflammatory responses, reversed by APN administration.[7] A study has shown that an APN alleviates an excessive systemic inflammation in the liver by suppressing MCP-1.[8] Simultaneously, a previous study provided evidence that the effects of APN on promoting preadipocyte differentiation under inflammatory conditions via anti-inflammation and antioxidative stress may be regulated by the PPAR γ/Nnat/NF-κB signaling pathway.[9] However, how hypoadiponectinemia contributes to vascular inflammation remains unclear.

APPL1 has been shown to interact with many partners involved in various signaling pathways mediating apoptosis, cell survival, cell proliferation, and chromatin remodeling.[10] Recent studies from other investigators demonstrated that APPL1 plays a critical role in APN signaling.[10–12] However, molecular signaling mechanisms mediating APPL1 vascular anti-inflammation have not been identified.

Therefore, the objectives of the current study were (1) to determine whether APPL1 is involved in APN-mediated vascular anti-inflammation and (2) to investigate the potential molecular mechanisms responsible for attenuating HG/HL-induced vascular inflammation.

[1]Department of Physiology & Pathophysiology, School of Basic Medical Sciences, Capital Medical University, Beijing 100069, P. R. China

[2]Medical Oncology Department, Pediatric Oncology Center, Beijing Children's Hospital, Capital Medical University, National Center for Children's Health, Beijing Key Laboratory of Pediatric Hematology Ocology, Key Laboratory of Major Diseases in Children, Ministry of Education, Beijing 100045, P. R. China

[3]Department of Ultrasound, Beijing Anzhen Hospital, Capital Medical University, Beijing Institute of Heart Lung and Blood Vessel Diseases, Beijing 100029, P. R. China

[4]Beijing Key Laboratory of Metabolic Disturbance Related Cardiovascular Disease, Beijing 100069, China

[5]Beijing Anzhen Hospital, Capital Medical University, Beijing Institute of Heart, Lung and Blood Vessel Diseases, Beijing 100029, P. R. China

[6]Department of Ophthalmology, Beijing Anzhen Hospital, Capital Medical University, Beijing 100029, China

[7]Department of Emergency Medicine, Thomas Jefferson University, Philadelphia, PA 19107, USA

[8]Lead contact

*Correspondence: annahhdu820@mail.ccmu.edu.cn (Y.D.), liuhr2000@ccmu.edu.cn (H.L.)

https://doi.org/10.1016/j.isci.2023.106428

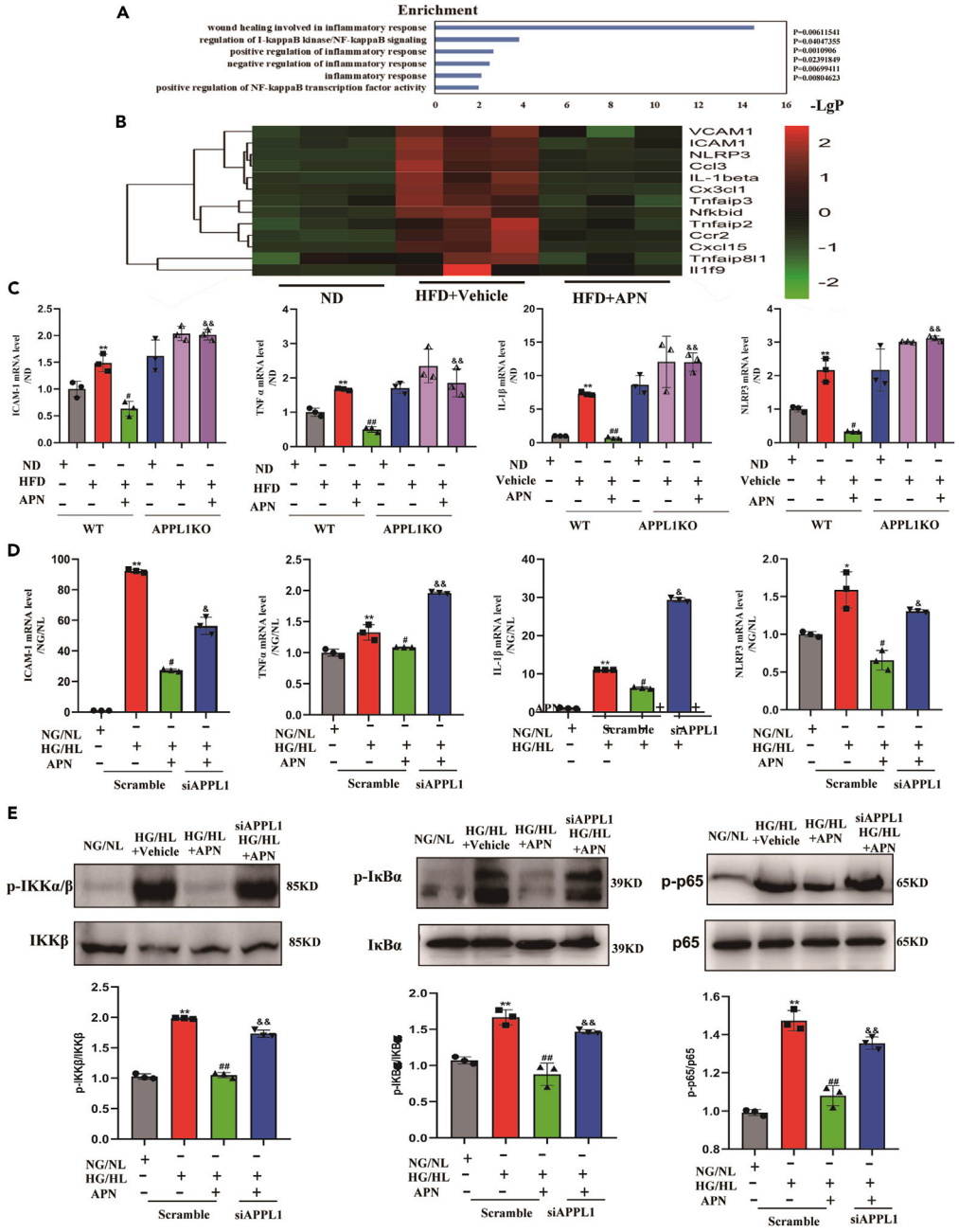

Figure 1. Adiponectin's anti-inflammation effect is APPL1 dependent

(A) Inflammation pathways regulated by differentially expressed genes; (B) Heatmap demonstrating the 13 inflammatory genes(promoted by HFD, inhibited by APN) involved in all inflammatory signaling; (C) Real-time PCR demonstrating mRNA levels of ICAM-1, TNF-α, IL-1β, and NLRP3 are significantly increased in aortic vessels from diabetic mice, whereas treatment with APN normalized their mRNA levels, an effect abolished by APPL1KO mice (N = 3, $^{**}p < 0.01$ vs. ND; $^{\#}p < 0.05$, $^{\#\#}p < 0.01$ vs. HFD+vehicle; $^{\&\&}p < 0.01$ vs. Scramble+HFD+APN); (D) The mRNA levels of ICAM-1, TNF-α, IL-1β, and NLRP3 are significantly increased in HUVECs exposed to HG/HL for 72 h, whereas treatment with APN for 24 h inhibited their mRNA levels in APPL1-dependent fashion(N = 3, independent experiments/group (N = 3, $^{*}p < 0.05$, $^{**}p < 0.01$ vs. NG/NL; $^{\#}p < 0.05$, $^{\#\#}p < 0.01$ vs. HG/HL + vehicle; $^{\&}p < 0.05$, $^{\&\&}p < 0.01$ vs. Scramble+HFD+APN); (E) APN treatment inhibited the activation of NF-κB pathway in HG/HL HUVECs, an effect abolished by APPL1 knockdown. (N = 3, $^{*}p < 0.05$, $^{**}p < 0.01$ vs. NG/NL; $^{\#}p < 0.05$, $^{\#\#}p < 0.01$ vs. HG/HL + vehicle; $^{\&}p < 0.05$, $^{\&\&}p < 0.01$ vs. Scramble+HG/HL + APN). Data are represented as mean ± SEM. Abbreviations: ND, normal diet; HFD, high fat diet; NG/NL, normal medium; HG/HL, high glucose/high lipid medium; APN: Adiponectin.

RESULTS

Adiponectin's anti-inflammation effect is APPL1 dependent

To identify vascular inflammatory signaling molecules that are stimulated by a high-fat diet (HFD) and suppressed by APN in a nonbiased fashion, wild-type[13] (WT) mice were maintained to feed normal or HFD for 12 weeks. 12 weeks after HFD, animals were randomized to obtain a vehicle or APN treatment for two additional weeks. Aortas were isolated and prepared for transcriptome analysis. Compared with normal diet (ND), 1,142 genes were significantly upregulated (Fold change > 2, FDR < 0.05) in HFD aortic vessels. 3,802 genes were significantly downregulated by APN administration in HFD mice compared to vehicle. Of these, 1,997 genes overlapped with those upregulated by HFD. To identify inflammatory genes inhibited by APN, GO functional annotation analysis was performed. Many inflammatory signaling pathways are listed in the GO analysis (Figure 1A). Further analysis identified 13 genes (*VCAM1, ICAM1, NLRP3, CCL3, IL-1β, Cx3cl1, Tnfaip3, Nfkbid, Tnfaid2, Ccr2, Cxcl15, Tnfaip8i1*, and *Il1f9*) were involved in APN's anti-inflammatory response by heatmap diagram analysis (Figure 1B). Among these genes, the results from real-time PCR exhibited that mRNA levels of ICAM-1, TNF-α, IL-1β, and NLRP3 were critically promoted in the aortas of HFD mice and inhibited by APN treatment (Figure 1C). To identify the involvement of APPL1 in APN gene regulation, APPL1KO mice were constructed (Figure S2). Compared with WT mice, the mRNA levels of ICAM-1, TNF-α, IL-1β, and NLRP3 were significantly upregulated in APPL1KO mice. And simultaneously, APPL1KO mice were fed with HFD and treated with APN. The results demonstrate that APN failed to inhibit the mRNA levels of ICAM-1, TNF-α, IL-1β, and NLRP3 in HFD-fed APPL1KO mice (Figure 1C), suggesting that APPL1 is essential for vascular endothelial inflammation inhibited by APN.

The aorta is composed of complex cellular types. In order to identify HFD-promoted and APN-inhibited genes via APPL1 signaling specific to vascular endothelial cells (ECs), human umbilical vein endothelial cells (HUVECs) were used to conduct the next experiments. The results showed that the mRNA levels of ICAM-1, TNF-α, IL-1β, and NLRP3 were significantly increased in diabetic ECs compared to normal ECs. Treatment with APN for 24 h inhibited their mRNA levels in an APPL1-dependent fashion (Figures 1D and S3). We also found that APPL1 is required for the inhibition of the NF-κB signaling pathway mediated by APN in HUVECs (Figure 1E). Simultaneously, the expression of ICAM-1 was significantly increased in diabetic aortic vessels and HG/HL cells compared to normal aortic vessels and vehicle group. Treatment with APN inhibited its expression in an APPL1-dependent manner (Figure S4). Taken together, these results presented in Figure 1 demonstrate that APN played a key role in HG/HL-induced vascular inflammation in an APPL1-dependent fashion.

Canonical Wnt/β-catenin activation mediates APN-induced anti-inflammation effect

Having demonstrated that APN treatment inhibited multiple inflammatory genes upregulated by HFD in an APPL1-dependent fashion, we attempted to discern responsible molecular signaling pathways. First, pathway analysis of differentially expressed genes (DEGs) was conducted to identify the signaling pathways most likely responsible for APN-mediated vasculoprotection. The results revealed that the canonical Wnt/β-catenin pathway genes exhibited the greatest enrichment (Figure 2A). We next determined total and active β-catenin protein levels *in vivo*. Amazingly, APN significantly increased the levels of total and active (non-phosphorylated) β-catenin in HFD-fed WT mice, but it had no effect on HFD-fed APPL1KO mice (Figure 2B). The nuclear localization of β-catenin is the defining step in Wnt/β-catenin pathway activation. Therefore, the cytoplasm and nuclear extracts of HUVECs were isolated to determine whether the nuclear translocation of β-catenin occurred. As shown in Figures 2C and 2D, APN treatment clearly increased active β-catenin expression in a nuclear fraction in cells transfected with scrambled siRNA, an effect nullified in cells transfected with siAPPL1, suggesting that APN promoted β-catenin nuclear translocation. At the same time, the nuclear translocation of β-catenin was determined by IF staining. The result showed that the nuclear localization of β-catenin was significantly decreased in HG/HL cells compared to vehicle group. Treatment with APN promoted its nuclear localization in an APPL1-dependent manner (Figure S5). These results indicate that APN administration activated the Wnt/β-catenin signaling pathway in an APPL1-dependent fashion.

Reptin is responsible for the activation of Wnt/β-catenin pathway mediated by APN in an APPL1-dependent fashion

A previous report reported that reptin could bind to β-catenin in the cytoplasm, which prevents β-catenin nuclear translocation.[14] Moreover, reptin also interacts directly with APPL1.[15] To determine the role of reptin in Wnt/β-catenin activation mediated by APN, several experiments were performed. First,

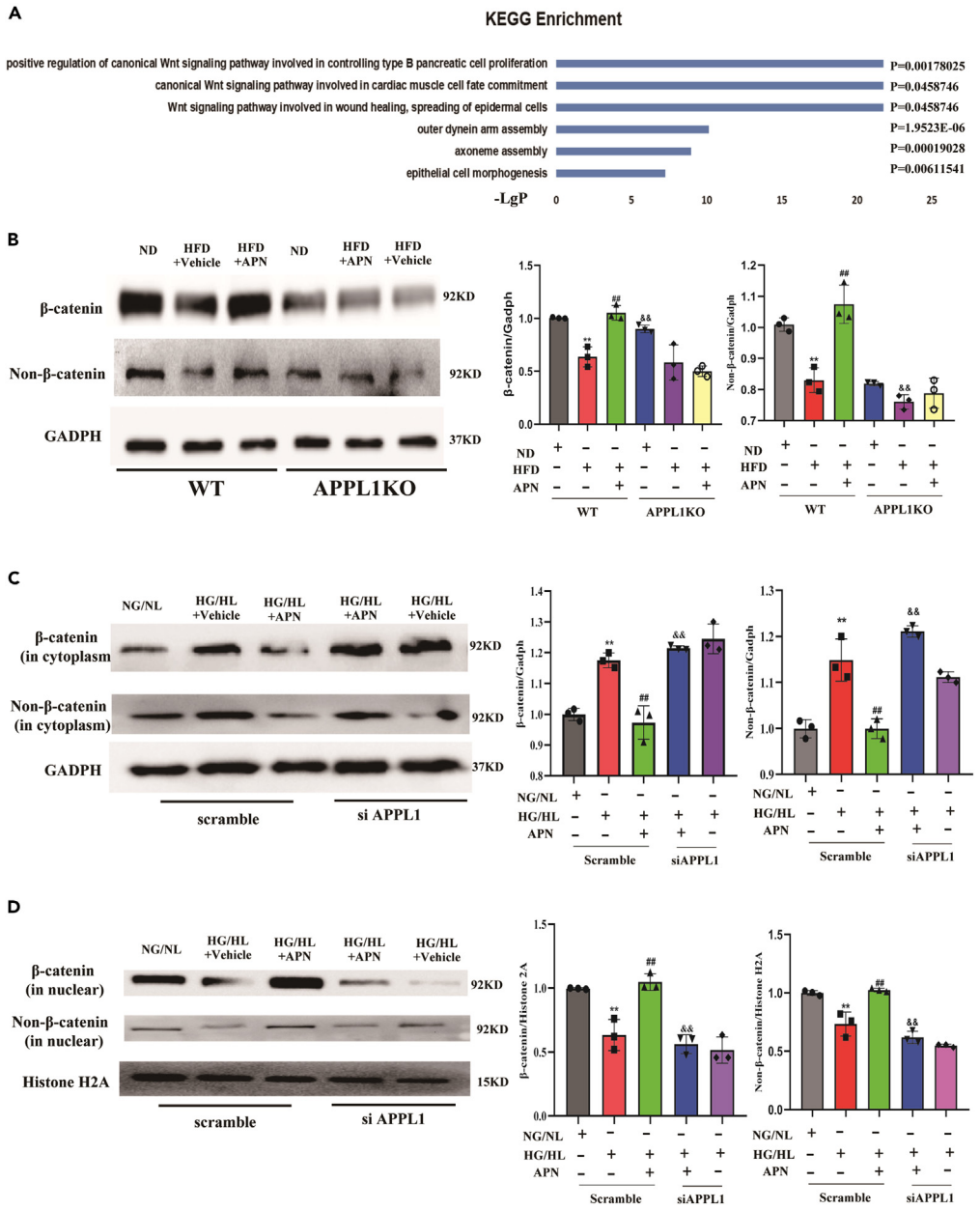

Figure 2. Canocical Wnt/β-catenin activation mediates APN-induced anti-inflammation effect

(A) KEGG pathway analysis; (B) Western blots and quantification of protein expression for β-catenin and non-β-catenin in aortic vessels from WT or APPL1KO mice. (N = 3, **$p < 0.01$ vs. ND; $^{\#\#}p < 0.01$ vs. HFD+vehicle; $^{\&\&}p < 0.01$ vs. Scramble+HFD+APN); (C and D) Western blots and quantification of β-catenin and non-β-catenin in HUVEC cytoplasm and nucleus. (Data are represented as mean ± SEM. N = 3, **$p < 0.01$ vs. NG/NL; $^{\#\#}p < 0.01$ vs. HG/HL + vehicle; $^{\&\&}p < 0$ 0.01 vs. Scramble+HG/HL + APN).

co-immunoprecipitation analysis was conducted to detect APPL1/reptin and reptin/β-catenin interaction. The results demonstrated that APN treatment markedly increased APPL1/reptin complex formation in a time-dependent manner (Figure 3A), but it inhibited reptin/β-catenin interaction (Figure 3B). Next, to further explore how APN regulates APPL1/reptin or reptin/β-catenin complex, BLI analysis was employed to determine the kinetics of the reptin-APPL1 and reptin-β-catenin complex after APN treatment. In this assay, we found that both APPL1/reptin and reptin/β-catenin complex has a high affinity (Figures S6A and S6B). APN administration promoted the association and slowed the dissociation of reptin and

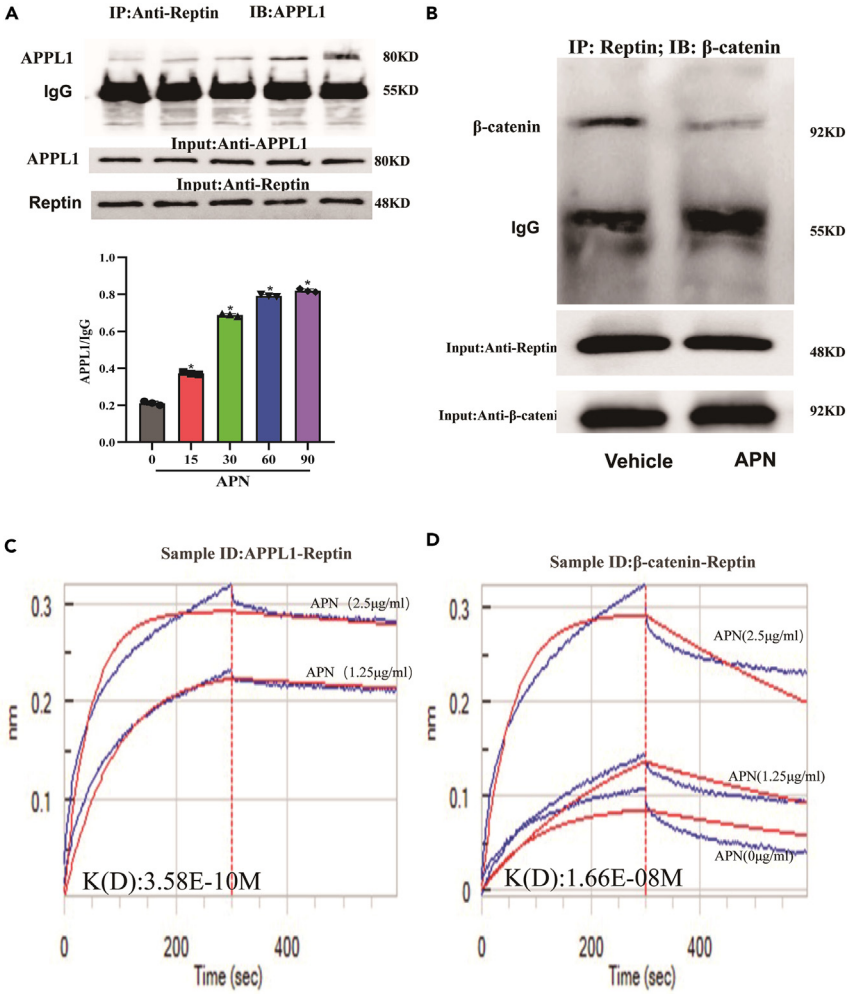

Figure 3. Reptin is responsible for the activation of Wnt/β-catenin pathway mediated by APN in an APPL1-dependent fashion

Co-immunoprecipitation demonstrating APN treatment (5 μg/ml) markedly increased APPL1/reptin complex formation as a time-dependent manner (A) (Data are represented as mean ± SEM. N = 3, **p < 0.01 vs. time 0), but it inhibited reptin/β-catenin interaction (B).

(C and D) Bio-layer interferometry (BLI) technique was performed to detect the binding and affinity of APPL1/β-catenin for reptin in APN treatment. The real-time binding curves are shown as blue lines, while the red lines indicate the global fits generated by fitting the blue line using 1:1 Langmuir binding model with mass transport limitation using the Scrubber software.

APPL1 (Kd: 7.46E-09M vs. 3.58E-10M) (Figures 3C and S6A). However, the interaction of reptin and β-catenin slightly decreased with adiponectin treatment (Kd: 3.08E-08M vs. 1.66E-08M) (Figures 3D and S6B). Thirdly, we used fluorescence resonance energy transfer (FRET) analysis to confirm the proteins interaction conclusion in living cell line. FRET analysis was employed to determine the interaction of the reptin-β-catenin complex after APN treatment. As shown in Figure S7A, FRET was detected by confocal microscopy between a fluorophore pair, CFP as donor and YFP as acceptor, which shares the character to allow fluorescence resonance energy transfer. Acceptor (YFP) bleaching protocol was applied to calculate the FRET efficiency. The left group of images shows a control cell co-stained with CFP-reptin and YFP-β-catenin that underwent an acceptor bleaching protocol. Both the pre- and post-bleaching images were presented on the top and middle panels. FRET image was generated by subtraction of fluorescent intensity in the pre-bleaching image from that in the post-bleaching image of CFP-reptin labeling. The overlaid images show the colocalization of both reptin and β-catenin detected under different protocols. As shown in FRET image, there was very high FRET detected under control condition. The right images show a APN-stimulated

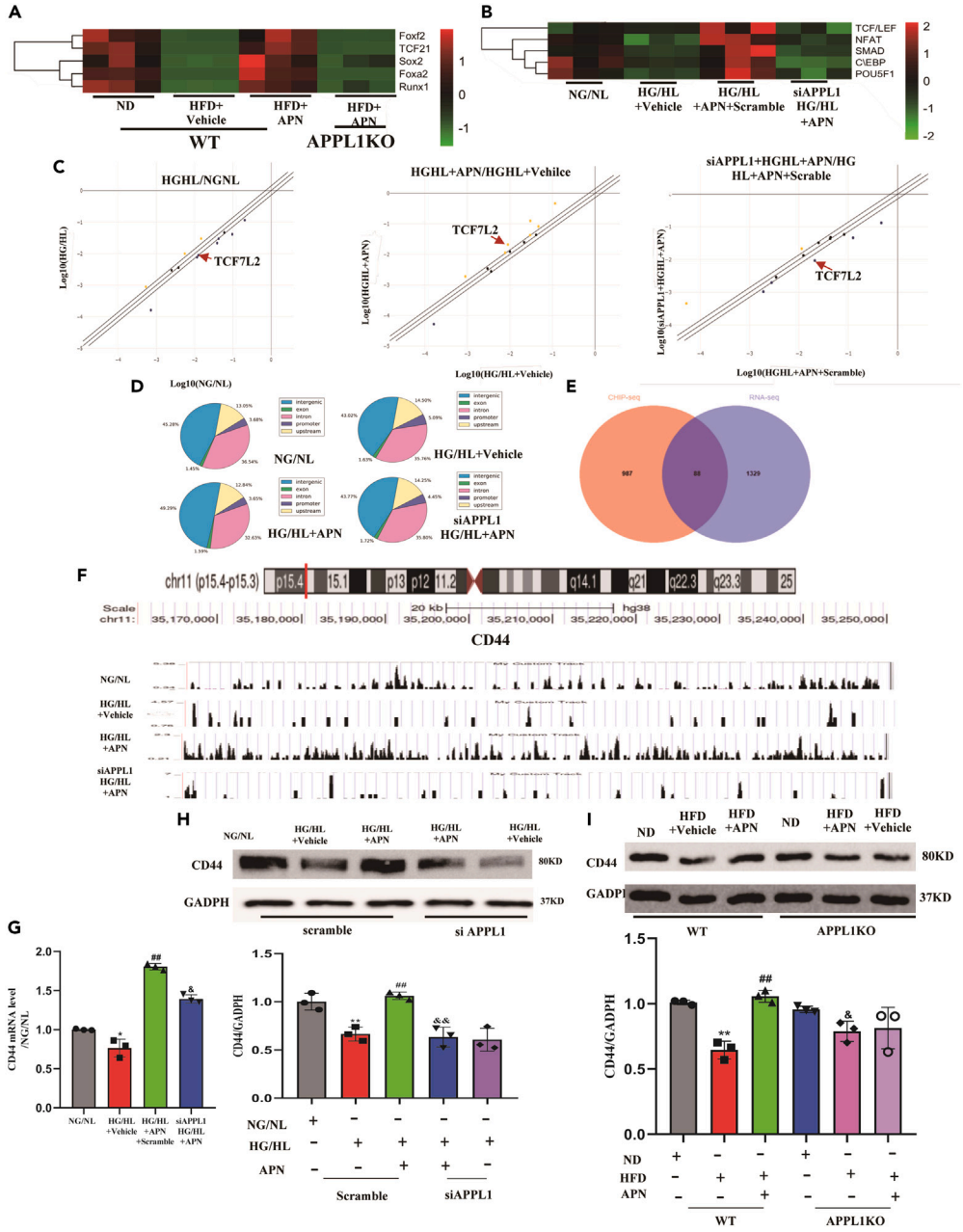

Figure 4. CD44 is a novel APN-APPL1-β-catenin downstream target gene

(A) 5 transcription factors involved in the Wnt/β-catenin pathway that is suppressed by HFD, rescued by APN and blocked by APPK1KO; (B) The activity of transcription factors was detected by transcription factor (TF) profiling array. Heatmap demonstrating the 5 upregulated transcription factors in HG/HL with APN in HUVEC nuclues; (C) Scatterplots showing APPL1 differentially Wnt/β-catenin pathway-related, APN-regulated transcription factors identified by the human transcription factor RT^2 profiler PCR array. Shown are the relative changes in gene expression accordingly to $2^{-\Delta\Delta CT}$ method with normalization to the average expression level of 5 housekeeping genes (Actb, B2m, Gapdh, Gusb, and Hsp90ab1). Yellow circles: genes upregulated >1.2-fold; blue circles: genes downregulated >1.2-fold; black circles: genes with <1.2-fold change.

(D) CHIP-seq was performed with an TCF antibody. Chart demonstrated percent of peaks within (E) TCF-binded genes identified in the CHIP dataset (left circle) were overlaid upon genes exhibiting APN-mediated APPL1-depedent expression in RNA-seq analysis (right circle) using HUVECs. 88 genes were present in both datasets.

(F) Map of CD44 locus revealing TCF binding in APN/APPL1 signaling; aligned reads were visualized by UCSC Genome Browser on Human. The signal is represented with black peaks in different groups respectively.

Figure 4. *Continued*

(G) Real-time PCR was performed to analyze CD44 mRNA levels (*$p < 0.05$ vs ND; $^{\#\#}p < 0.01$ vs. HFD+vehicle; $^{\&}p < 0.05$ vs. Scramble+HFD+APN). Western blot was used to assess the protein levels of CD44 *in vitro* (H) and *in vivo* (I). (**$p < 0.01$ vs. NG/NL; $^{\#\#}p < 0.01$ vs. HG/HL + vehicle; $^{\&}p < 0.05$,$^{\&\&}p < 0.01$ vs. Scramble+HG/HL + APN). Data are presented as mean ± SEM.

cell that underwent the same FRET protocol. A weaker FRET image was detected in these APN-treated HUVECs, demonstrating that energy transfer did not occur between reptin and β-catenin. As summarized in Figure S7B, the FRET efficiency between reptin and β-catenin were significantly decreased upon APN stimulation compared to control group (n = 3). The data showed that APN administration promoted reptin/APPL1 complex formation and partly inhibited reptin/β-catenin interaction, suggesting that reptin is involved in the APN-activated Wnt/β-catenin signaling pathway.

CD44 is a novel APN-APPL1-β-catenin downstream target gene

Previous studies demonstrated that nuclear-translocated β-catenin form a complex with TCF/LEF, SOX2, NFAT, and other transcription factors to regulate the expression of downstream genes.[16] To further clarify whether APN-stimulated, APPL1-mediated β-catenin nuclear translocation can activate transcription factors, we employed three separate approaches to obtain the most conclusive evidence. First, we utilized the RNA-seq technique. The results showed that APN treatment rescued five transcription factors downregulated by HFD in an APPL1-dependent fashion (*Foxf2, TCF21, Sox2, Foxa2,* and *Runx1*) (Figure 4A). Second, we employed a transcription factor activity detection kit to determine APN-activated, APPL1-mediated transcription factors. As shown in Figure 4B, the activity of 5 transcription factors was down-regulated by HG/HL, but activated by APN in an APPL1-dependent manner (TCF/LEF, NFAT, SMAD, C/EBP, and POU5F1). Third and finally, RT^2 Profiler human transcription factor PCR Array was performed. Among 13 human transcription factors known to be critical in the Wnt/β-catenin signaling pathway, 7 transcription factors were significantly downregulated in EC treated by HG/HL. APN administration upregulated 7 transcription factors, of which 4 (*NFATC4, TCF7L2, TP53,* and *JUN*) overlap with transcription factors downregulated by HG/HL. Five transcription factors were significantly downregulated in APPL1 knockdown EC. Venn overlapping analysis identified only one transcription factor TCF7L2 (the member of the TCF/LEF family) downregulated by HG/HL and rescued by APN treatment in an APPL1-dependent fashion (Figure 4C). Combining the findings from these three approaches, we focused on TCF/LEF transcription factor.

To further investigate target genes regulated by TCF/LEF in APN-stimulated, APPL1-mediated β-catenin signaling pathway, two strategies were utilized to identify the target genes for APN/APPL1/β-catenin/TCF downstream signaling. First, transcriptome analysis was reanalyzed to identify target genes. The analysis identified there were 1417 DEGs in APN-upregulated APPL1-mediated genes in the diabetic state. Second, to further investigate target genes regulated by TCF/LEF in APN/APPL1 signaling, TCF/LEF CHIP-seq was performed (Figure 4D). We identified 1,075 TCF/LEF target genes selectively enriched in APN-stimulated, APPL1-related differential genes. To narrow the number of TCF/LEF-mediated genes in APN/APPL1 signaling, we performed a Venn diagram analysis on our generated RNA-sequencing results combined with CHIP-seq analysis. 88 differentially expressed genes were overlapped in RNA-seq and CHIP-seq (Figure 4E). Combining the findings from these two strategies, we focused on CD44 genes. CHIP-seq analysis revealed a significant TCF-binding promoter in the CD44 gene promoted by APN treatment in an APPL1-dependent manner (Figure 4F). Studies have demonstrated TCF/LEF can promote CD44 expression as a transcription factor by CHIP-qPCR.[17–19] At the same time, the mRNA levels of CD44 were significantly inhibited in ECs treated by HG/HL. APN treatment only rescued CD44 mRNA expressions in cells transfected with scrambled siRNA, an effect nullified in cells transfected with siAPPL1 (Figure 4G). Simultaneously, APN treatment restored the expression of CD44 in an APPL1-dependent fashion (Figure 4H). Consistent with these *in vitro* findings, the protein level of CD44 was significantly reduced in HFD-fed mice compared to ND-fed WT mice, and APN administration upregulated CD44 expression in WT aortic tissue, an effect lost in APPL1KO mice (Figure 4I). Taken together, these results suggest that CD44 is the primary target gene activated by APN/APPL1/β-catenin/TCF/LEF signaling.

CD44 is critically involved in APN-stimulated, APPL1-mediated vascular anti-inflammatory effects

To determine the role of CD44 in APN-stimulated, APPL1-mediated vascular endothelial inflammatory effect, RNA interference technique was used to reduce the level of CD44 in ECs (Figure S8). The data show

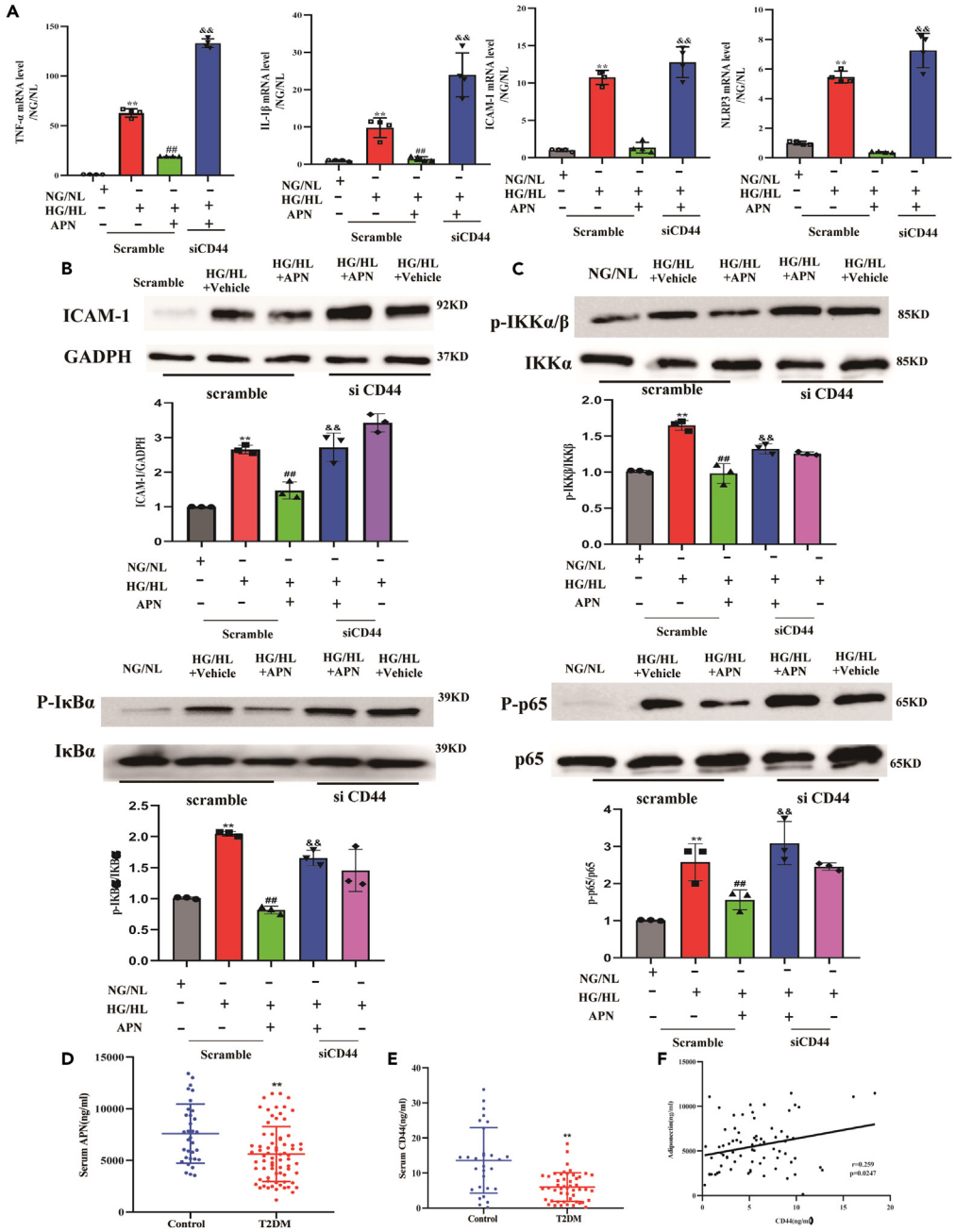

Figure 5. CD44 is critically involved in APN-stimulated, APPL1-mediated vascular anti-inflammatory effects

(A) Real-time PCR analysis of mRNA level for inflammatory factors in HUVEC (N = 4, **p < 0.01 vs. NG/NL; $^{\#\#}$p < 0.01 vs. HG/HL + vehicle; $^{\&\&}$p < 0.01 vs. Scramble+HG/HL + APN); (B and C) Western blots and quantification of protein expression for ICAM-1 and NF-κB pathway in HUVEC cell lysis. (N = 3, **p < 0.01 vs. NG/NL; $^{\#\#}$p < 0.01 vs. HG/HL + vehicle; $^{\&\&}$p < 0.01 vs. Scramble+HG/HL + APN).

(D and E) Serum titers of APN and CD44 in healthy subjects and patients with diabetes; (F) Serum CD44 concentrations were positively correlated with APN (n = 74, r = 0.259, p = 0.0247). Data are presented as mean ± SEM or median ± interquartile range (25th–75th percentile). OD indicates optical density.

that the inflammatory molecules whose downregulation by APN were blocked by CD44 knockdown (Figure 5A). Simultaneously, the inhibitory effect of APN on the protein levels of ICAM-1 disappeared after CD44 knockdown (Figure 5B). As illustrated in Figure 5C, HG/HL significantly induced IKK, IκB, and p65

phosphorylation. APN treatment inhibited phosphorylation levels of IKK, IκB, and p65, an effect nullified in cells transfected with siCD44.

To obtain direct evidence supporting the involvement of CD44 in the APN's anti-inflammatory effect, the plasma levels of CD44 and APN were determined in humans by ELISA. A total of 104 (T2DM vs. Control, 74 vs. 30) subjects were enrolled in this study. Demographic data and baseline clinical and biochemical characteristics are presented in Table S1. Statistical analysis showed that the levels of FBG were increased. Serum titers of APN were markedly decreased in diabetes compared with healthy controls as previously reported (5550.963 [IQR,2831.599–8270.327] versus 8255.391 [IQR,4345.461–12165.321] ng/mL; $p < 0.001$, Figure 5D). Notably, serum CD44 levels in the diabetic group were significantly lower than in the healthy group (5.6750 ng/mL [IQR, 1.932–9.418] versus 14.8518 ng/mL [IQR, 3.7699–25.9337]; $p < 0.01$, Figure 5E). Univariate logistics regression analysis indicated that serum CD44 in the T2DM group was positively correlated with APN (Figure 5F). At the same time, we identified that the serum CD44 levels were lower in diabetes via Western blot (Figure S9).

As the final step to prove the pathogenic role of CD44 reduction in endothelial inflammatory response inhibited by APN, the effect of CD44 supplementation on vascular inflammatory response induced by HFD was determined. Previous studies demonstrated that CD44 activates its downstream signaling via the C terminal domain (286-500aa).[20] A polypeptide (225–500) containing the active domain of CD44 was administered to HFD animals (Figure S10). As shown in Figure 6A, compared to the vehicle group, CD44 polypeptides administration markedly inhibited the mRNA levels of ICAM-1, TNF-α, and NLRP3 in HFD-fed WT mice as well as HFD-fed APN KO mice. Similarly, treatment with CD44 polypeptides significantly decreased expressions of ICAM-1 and NF-κB protein in the aortic vessels from HFD-fed WT mice (Figures 6B and 6C), HFD-fed APN KO mice (Figures 6D and 6E) and HFD-fed APPL1KO mice (Figures S11A and S10B). Taken together, these results present that CD44 plays an important role in the HFD-induced vascular endothelial cells inflammation effect.

DISCUSSION

A high incidence of cardiovascular complications persists in diabetes although intensive glucose control. Here, we provide evidence that APN plays a critical role in the vascular inflammation effect induced by HG/HL in an APPL1-dependent manner. Mechanistically, our findings implicate APN-attenuated hyperglycemia-induced inflammation by APPL1/WNT/β-catenin/CD44 signaling axis. We also show that CD44, as a target gene of APN, attenuated diabetic inflammation *in vitro* and *in vivo*.

CD44 antigen is a cell-surface glycoprotein involved in cell-cell interactions, cell adhesion, and migration.[21] CD44 is expressed in a large number of mammalian cell types.[22] CD44 is a receptor for hyaluronic acid and can also interact with other ligands, such as osteopontin, collagens, and matrix metalloproteinases (MMPs).[23] Several studies have suggested that CD44 is identified as a biomarker of a variety of cancers, which participated in cancer cell proliferation and invasion.[24] Current therapeutic strategies include neutralizing antibody,[25] peptide mimetics,[26] aptamers,[27] natural compounds[28] that suppress the expression of CD44. Recent studies demonstrate that CD44 maintains pulmonary vascular endothelial barrier integrity *in vivo* model.[29] Given the currently available information regarding the functional difference of CD44, its role in diabetes is still limited and far from conclusive. In this study, we demonstrate for the first time that CD44 plays an irreplaceable role in the adiponectin-inhibited diabetic vascular inflammation effect. In the past, signal transduction was considered to be a linear cascade involving protein-protein interactions, protein modifications, and small signaling molecules.[30] Amazingly, we found CD44 located in an important position in the global signal transduction network of RNA sequence analysis (Figure S12). To obtain the most reliable evidence to clarify the role of CD44 in pertaining to diabetic vascular endothelial inflammation effect, two different models were employed. We first utilized a loss-of-function approach, demonstrating adiponectin-inhibited endothelial inflammation effect in a CD44-dependent manner. CD44 is traditionally considered a transmembrane protein. It has been reported that the C-terminal cytoplasmic domain (286-500aa) supports the binding of proteins with crucial functions in signaling transduction.[31] The cytoplasm of CD44 is the defining step in downstream pathway activation. To further identify the role of CD44 in the diabetic model, we next used a gain-of-function approach by administering CD44 polypeptides (Sangon Biotech, D622619, 225-500aa) to mice. We identify whether the CD44 polypeptides can be effective, the cytoplasm and membrane extracts of HUVECs were isolated to determine whether CD44 polypeptides (225-500aa) enter the cytoplasm. As shown in Figure S13, CD44 polypeptides treatment

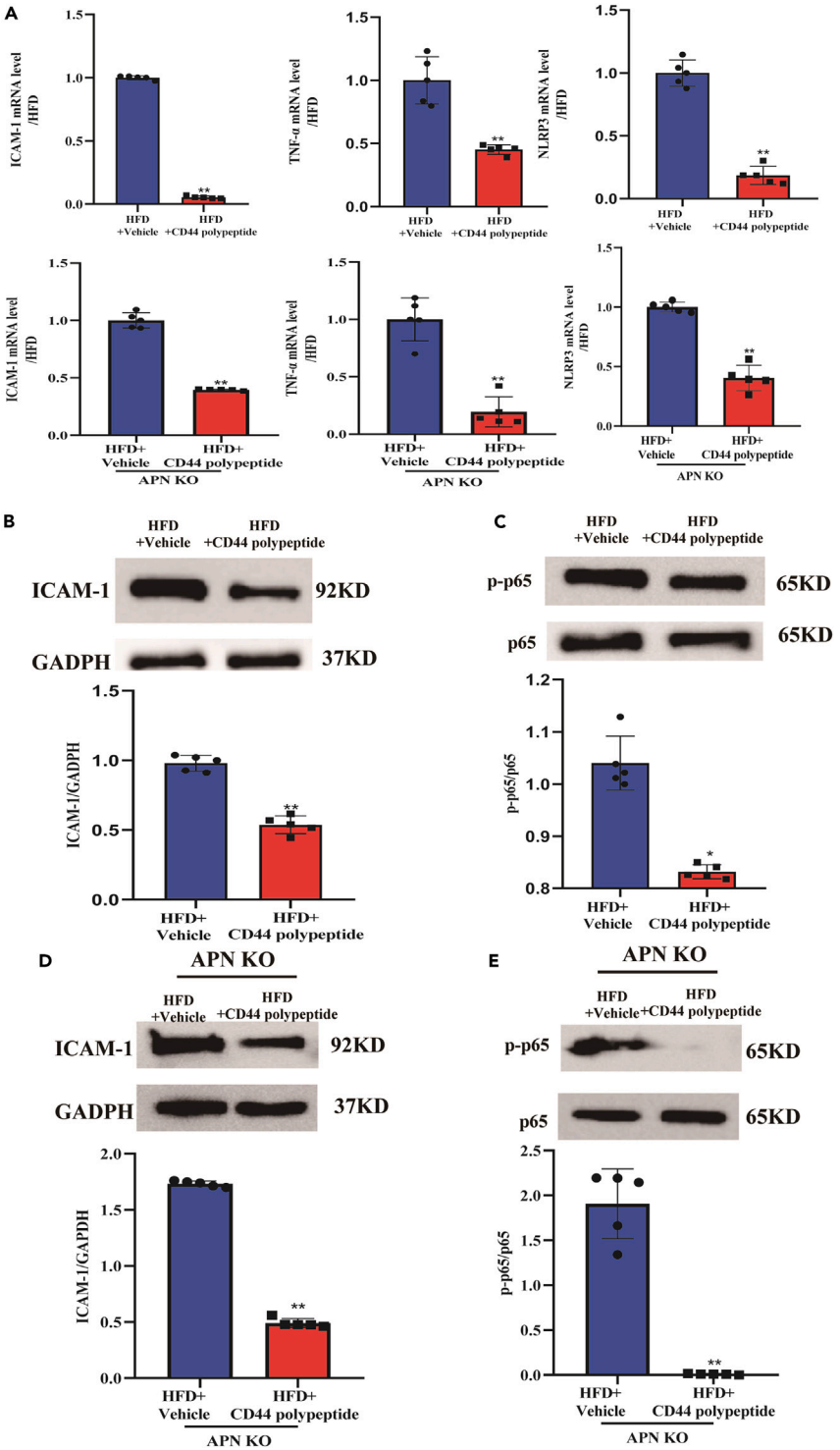

Figure 6. Administration of CD44 polypeptides prevented HFD-induced vascular inflammatory effect

(A) Real-time PCR analysis of mRNA level for inflammatory factors *in vivo* (N = 5, **p < 0.01 vs. HFD+Vehicle). Western blots and quantification of protein expression for ICAM-1 and NF-κB pathway in HFD-fed WT mice (B and C) or HFD-fed APN KO mice (D and E) (N = 5, *p < 0.05, **p < 0.01 vs. HFD+Vehicle). Data are presented as mean ± SEM.

clearly increased CD44 level in cytoplasm fraction in cells, suggesting that exogenous CD44 polypeptides may activate downstream pathways to suppress the inflammatory response. We also used CD44 polypeptides to treat HFD-fed mice, demonstrating that CD44 polypeptides attenuated diabetic vascular inflammation. Finally, we found that serum CD44 levels and APN levels were decreased in patients with diabetes compared to the healthy group, and CD44 concentration was positively correlated with APN level in the setting of diabetes. Collectively, we provide clear evidence that CD44 may represent a novel therapeutic approach against the diabetic vascular inflammatory effects.

It is well known that endothelial dysfunction caused by diabetes is an important risk factor for diabetic cardiovascular disease and related mortality.[32] The endothelium has emerged as the key regulator of vascular homeostasis in that it has not merely a barrier function but also acts as an active signal transducer for circulating influences that modify the vessel wall phenotype.[33] Recent research on how to inhibit diabetic vascular endothelial damage has become a hot spot. The emerging evidence shows that inflammatory effect is the key to the development of endothelial injury and diabetic vasculopathy.[34] Both clinical observations and basic science studies support that increased adiponectin levels have correlated with improved endothelial function.[35] It has been reported that adiponectin enhances the production of nitric oxide, suppresses the production of reactive oxygen species, and protects cells from inflammation that results from exposure to high glucose levels or tumor necrosis factor through activation of AMP-activated protein kinase and cyclic AMP-dependent protein kinase (also known as protein kinase A) signaling cascades.[36] However, critical questions regarding the mechanisms of APN's vasculoprotection remain incompletely understood. We elucidated that APN/APPL1/Wnt/β-catenin signaling axis and subsequent CD44 promotion is a novel mechanism mediating the anti-inflammatory effect in endothelial cells.

APPL1, an adapter protein containing an NH_2-terminal BAR domain, a PH domain, a COOH-terminal PTB, and a leucine zipper motif,[37] has been shown to be involved in the regulation of cell proliferation and in the crosstalk between the adiponectin signaling and insulin signaling pathways.[38] APPL1 binds with many other proteins, including AKT2, adiponectin receptors, and proteins of the NuRD/MeCP1 complex.[39] Previous studies corroborated that APPL1 functions downstream of APN in various tissue and cell types[38] and bind to the cytoplasmic tails of AdipoR1 and AdipoR2 in response to adiponectin,[40] thereby activating AMPK and eNOS and resulting in the production of NO in endothelial cells.[41] However, whether APPL1 may participate in APN's endothelial anti-inflammatory effect has not been previously investigated in the diabetic model. The present study provides the first evidence that APN inhibited expressions of ICAM-1, NLRP3, Il-1, TNF-α, and NF-κB in an APPL1-dependent manner in both *in vivo* and *in vitro* models. Our data demonstrate that APPL1 is involved in the anti-inflammatory effect of APN in HG/HL endothelial cells.

The Wnt/β-catenin pathway is an essential regulator of development and homeostasis in many tissues.[42] Signaling is initiated by secreted Wnt ligands, which bind frizzled (FZD) membrane receptors on cells within close proximity to trigger Wnt response.[43] Study has demonstrated that the endosomal proteins APPL1 and APPL2 are novel activators of beta-catenin/TCF-mediated transcription.[15] Simultaneously, related studies have identified exosome-mediated activation of the OPN/CD44 axis plays a key role in renal fibrosis, which is controlled by β-catenin[44] In this report, we proposed a novel explanation regarding Wnt/β-catenin pathway is involved in APN-mediated, APPL1-dependent vascular anti-inflammatory effect. We found APN increased the expressions of total β-catenin and active β-catenin in *in vivo* model in an APPL1-dependent manner. Simultaneously, APN promoted active β-catenin translocation, leading to β-catenin-dependent transcriptional activation. Surprisingly, we recovered that adiponectin promoted the complex formation of reptin-APPL1 and partly inhibited the interaction of reptin-β-catenin by biofilm interference technology. Additionally, APN did not increase the expression of reptin, but APPL1 indeed promoted the expression of reptin *in vivo* and *in vitro* (Figures S14A and S14B). Collectively, the Wnt/β-catenin pathway is involved in the APN-inhibited vascular endothelial inflammation effect in an APPL1-mediated fashion.

In summary, our current findings provide supporting evidence that APN inhibits diabetic vascular inflammatory effect by WNT/β-catenin pathway activation and downstream target gene activation of CD44 in an APPL1-dependent manner. Decreased serum CD44 and adiponectin levels play a causative role in diabetic endothelium inflammatory effects in diabetes. Our data suggest positive modulation of endothelial CD44 may represent a novel therapeutic approach against the diabetic-induced vascular endothelial inflammatory effect.

Limitations of the study

This study focuses on identifying the mechanisms responsible for APN-mediated anti-inflammation and searching the downstream potential targets. The validation of the target gene was achieved in cellular models and animal models but the potential protective mechanisms of the target gene would need further investigation using animal models and cell models.

STAR★METHODS

Detailed methods are provided in the online version of this paper and include the following:

- KEY RESOURCES TABLE
- RESOURCE AVAILABILITY
  - Lead contact
  - Materials availability
  - Data and code availability
- EXPERIMENTAL MODEL AND SUBJECT DETAILS
  - Human subjects
  - Type 2 diabetic mice model
  - Cell lines
- METHOD DETAILS
  - Co-immunoprecipitation and western blot analysis
  - Small interfering RNA transfection
  - Cell compartment isolation
  - Transcription factor (TF) profiling array
  - RNA sequencing
  - Bioinformatics analysis
  - RT^2 Profiler PCR array human transcription factors and quantitative Real-Time PCR (qRT-PCR) analysis
  - Enzyme-linked immunosorbent assay (ELISA)
  - BLI binding array
  - Fluorescence resonance energy transfer (FRET) analysis
  - CHIP-sequencing and peak finding
- QUANTIFICATION AND STATISTICAL ANALYSIS

SUPPLEMENTAL INFORMATION

Supplemental information can be found online at https://doi.org/10.1016/j.isci.2023.106428.

ACKNOWLEDGMENTS

This work was supported by the National Natural Science Foundation of China (No. 82070370 and 81873464).

AUTHOR CONTRIBUTIONS

Conceptualization, Y.R.D. and Y.H.D.; Methodology, S.Z., Y.X., Y.W., W.Z., P.X., H.Z., and X.G.; Investigation, Y.R.D.,Y.H.D., and H.L.; Writing – Original Draft, Y.R.D. and Y.H.D.; Writing – Review & Editing, Y.R.D.,Y.H.D., and H.L.; Funding Acquisition, Y.H.D.; Resources, Y.Q., Y.W., and X.M.; Supervision, Y.H.D. and H.L.

DECLARATION OF INTERESTS

We, the authors, have a patent related to this work (No. ZL 202110749325.X).

Received: August 15, 2022
Revised: September 30, 2022
Accepted: March 13, 2023
Published: March 20, 2023

REFERENCES

1. Srikanth, V., Sinclair, A.J., Hill-Briggs, F., Moran, C., and Biessels, G.J. (2020). Type 2 diabetes and cognitive dysfunction-towards effective management of both comorbidities. The lancet. Lancet Diabetes Endocrinol. *8*, 535–545. https://doi.org/10.1016/s2213-8587(20)30118-2.

2. Ljubkovic, M., Gressette, M., Bulat, C., Cavar, M., Bakovic, D., Fabijanic, D., Grkovic, I., Lemaire, C., and Marinovic, J. (2019). Disturbed fatty acid oxidation, endoplasmic reticulum stress, and apoptosis in left ventricle of patients with type 2 diabetes. Diabetes *68*, 1924–1933. https://doi.org/10.2337/db19-0423.

3. Poznyak, A., Grechko, A.V., Poggio, P., Myasoedova, V.A., Alfieri, V., and Orekhov, A.N. (2020). The diabetes mellitus-atherosclerosis connection: the role of lipid and glucose metabolism and chronic inflammation. Int. J. Mol. Sci. *21*, 1835. https://doi.org/10.3390/ijms21051835.

4. Liu, G.Z., Liang, B., Lau, W.B., Wang, Y., Zhao, J., Li, R., Wang, X., Yuan, Y., Lopez, B.L., Christopher, T.A., et al. (2015). High glucose/High Lipids impair vascular adiponectin function via inhibition of caveolin-1/AdipoR1 signalsome formation. Free Radic. Biol. Med. *89*, 473–485. https://doi.org/10.1016/j.freeradbiomed.2015.09.005.

5. Kadowaki, T., Yamauchi, T., Kubota, N., Hara, K., Ueki, K., and Tobe, K. (2006). Adiponectin and adiponectin receptors in insulin resistance, diabetes, and the metabolic syndrome. J. Clin. Invest. *116*, 1784–1792. https://doi.org/10.1172/jci29126.

6. Choi, H.M., Doss, H.M., and Kim, K.S. (2020). Multifaceted physiological roles of adiponectin in inflammation and diseases. Int. J. Mol. Sci. *21*, 1219. https://doi.org/10.3390/ijms21041219.

7. Takemura, Y., Ouchi, N., Shibata, R., Aprahamian, T., Kirber, M.T., Summer, R.S., Kihara, S., and Walsh, K. (2007). Adiponectin modulates inflammatory reactions via calreticulin receptor-dependent clearance of early apoptotic bodies. J. Clin. Invest. *117*, 375–386. https://doi.org/10.1172/jci29709.

8. Ryu, J., Hadley, J.T., Li, Z., Dong, F., Xu, H., Xin, X., Zhang, Y., Chen, C., Li, S., Guo, X., et al. (2021). Adiponectin alleviates diet-induced inflammation in the liver by suppressing MCP-1 expression and macrophage infiltration. Diabetes *70*, 1303–1316. https://doi.org/10.2337/db20-1073.

9. Yang, W., Yuan, W., Peng, X., Wang, M., Xiao, J., Wu, C., and Luo, L. (2019). PPAR γ/Nnat/NF-κB Axis involved in promoting effects of adiponectin on preadipocyte differentiation. Mediators Inflamm. *2019*, 5618023. https://doi.org/10.1155/2019/5618023.

10. Deepa, S.S., and Dong, L.Q. (2009). APPL1: role in adiponectin signaling and beyond. Am. J. Physiol. Endocrinol. Metab. *296*, E22–E36. https://doi.org/10.1152/ajpendo.90731.2008.

11. Artimani, T., and Najafi, R. (2020). APPL1 as an important regulator of insulin and adiponectin-signaling pathways in the PCOS: a narrative review. Cell Biol. Int. *44*, 1577–1587. https://doi.org/10.1002/cbin.11367.

12. Wang, C., Xin, X., Xiang, R., Ramos, F.J., Liu, M., Lee, H.J., Chen, H., Mao, X., Kikani, C.K., Liu, F., and Dong, L.Q. (2009). Yin-Yang regulation of adiponectin signaling by APPL isoforms in muscle cells. J. Biol. Chem. *284*, 31608–31615. https://doi.org/10.1074/jbc.M109.010355.

13. Azziz, R., Carmina, E., Chen, Z., Dunaif, A., Laven, J.S.E., Legro, R.S., Lizneva, D., Natterson-Horowtiz, B., Teede, H.J., and Yildiz, B.O. (2016). Polycystic ovary syndrome. Nat. Rev. Dis. Primers *2*, 16057. https://doi.org/10.1038/nrdp.2016.57.

14. Kim, J.H., Kim, B., Cai, L., Choi, H.J., Ohgi, K.A., Tran, C., Chen, C., Chung, C.H., Huber, O., Rose, D.W., et al. (2005). Transcriptional regulation of a metastasis suppressor gene by Tip60 and beta-catenin complexes. Nature *434*, 921–926. https://doi.org/10.1038/nature03452.

15. Rashid, S., Pilecka, I., Torun, A., Olchowik, M., Bielinska, B., and Miaczynska, M. (2009). Endosomal adaptor proteins APPL1 and APPL2 are novel activators of beta-catenin/TCF-mediated transcription. J. Biol. Chem. *284*, 18115–18128. https://doi.org/10.1074/jbc.M109.007237.

16. MacDonald, B.T., Tamai, K., and He, X. (2009). Wnt/beta-catenin signaling: components, mechanisms, and diseases. Dev. Cell *17*, 9–26. https://doi.org/10.1016/j.devcel.2009.06.016.

17. Henderson, B.R., and Fagotto, F. (2002). The ins and outs of APC and beta-catenin nuclear transport. EMBO Rep. *3*, 834–839. https://doi.org/10.1093/embo-reports/kvf181.

18. Yu, W., Ma, Y., Shankar, S., and Srivastava, R.K. (2017). SATB2/β-catenin/TCF-LEF pathway induces cellular transformation by generating cancer stem cells in colorectal cancer. Sci. Rep. *7*, 10939. https://doi.org/10.1038/s41598-017-05458-y.

19. Mosimann, C., Hausmann, G., and Basler, K. (2009). Beta-catenin hits chromatin: regulation of Wnt target gene activation. Nat. Rev. Mol. Cell Biol. *10*, 276–286. https://doi.org/10.1038/nrm2654.

20. Goncalves, A., Dreffs, A., Lin, C.M., Sheskey, S., Hudson, N., Keil, J., Campbell, M., and Antonetti, D.A. (2021). Vascular expression of permeability-resistant Occludin mutant preserves visual function in diabetes. Diabetes *70*, 1549–1560. https://doi.org/10.2337/db20-1220.

21. Jothy, S. (2003). CD44 and its partners in metastasis. Clin. Exp. Metastasis *20*, 195–201. https://doi.org/10.1023/a:1022931016285.

22. Ma, L., Dong, L., and Chang, P. (2019). CD44v6 engages in colorectal cancer progression. Cell Death Dis. *10*, 30. https://doi.org/10.1038/s41419-018-1265-7.

23. Senbanjo, L.T., and Chellaiah, M.A. (2017). CD44: a multifunctional cell surface adhesion receptor is a regulator of progression and metastasis of cancer cells. Front. Cell Dev. Biol. *5*, 18. https://doi.org/10.3389/fcell.2017.00018.

24. Yan, Y., Zuo, X., and Wei, D. (2015). Concise review: emerging role of CD44 in cancer stem cells: a promising biomarker and therapeutic target. Stem Cells Transl. Med. *4*, 1033–1043. https://doi.org/10.5966/sctm.2015-0048.

25. Runnels, H.A., Weber, G.L., Min, J., Kudlacz, E.M., Zobel, J.F., Donovan, C.B., Thiede, M.A., Zhang, J., Alpert, R.B., Salafia, M.A., et al. (2010). PF-03475952: a potent and neutralizing fully human anti-CD44 antibody for therapeutic applications in inflammatory diseases. Adv. Ther. *27*, 168–180. https://doi.org/10.1007/s12325-010-0010-0.

26. Hauser-Kawaguchi, A., Luyt, L.G., and Turley, E. (2019). Design of peptide mimetics to block pro-inflammatory functions of HA fragments. Matrix Biol. *78–79*, 346–356. https://doi.org/10.1016/j.matbio.2018.01.021.

27. Pęcak, A., Skalniak, Ł., Pels, K., Książek, M., Madej, M., Krzemień, D., Malicki, S., Władyka, B., Dubin, A., Holak, T.A., and Dubin, G. (2020). Anti-CD44 DNA aptamers selectively target cancer cells. Nucleic Acid Ther. *30*, 289–298. https://doi.org/10.1089/nat.2019.0833.

28. Petukhov, D., Richter-Dayan, M., Fridlender, Z., Breuer, R., and Wallach-Dayan, S.B. (2019). Increased regeneration following stress-induced lung injury in bleomycin-treated chimeric mice with CD44 knockout mesenchymal cells. Cells *8*. https://doi.org/10.3390/cells8101211.

29. Isobe, S., Kataoka, M., Endo, J., Moriyama, H., Okazaki, S., Tsuchihashi, K., Katsumata, Y., Yamamoto, T., Shirakawa, K., Yoshida, N., et al. (2019). Endothelial-mesenchymal transition drives expression of CD44 variant and xCT in pulmonary hypertension. Am. J. Respir. Cell Mol. Biol. *61*, 367–379. https://doi.org/10.1165/rcmb.2018-0231OC.

30. Chen, J., Sagum, C., and Bedford, M.T. (2020). Protein domain microarrays as a platform to decipher signaling pathways and the histone code. Methods (San Diego, Calif.) *184*, 4–12. https://doi.org/10.1016/j.ymeth.2019.08.007.

31. Ponta, H., Sherman, L., and Herrlich, P.A. (2003). CD44: from adhesion molecules to signalling regulators. Nat. Rev. Mol. Cell Biol. *4*, 33–45. https://doi.org/10.1038/nrm1004.

32. Incalza, M.A., D'Oria, R., Natalicchio, A., Perrini, S., Laviola, L., and Giorgino, F. (2018). Oxidative stress and reactive oxygen species in endothelial dysfunction associated with cardiovascular and metabolic diseases. Vascul. Pharmacol. *100*, 1–19. https://doi.org/10.1016/j.vph.2017.05.005.

33. Shi, Y., and Vanhoutte, P.M. (2017). Macro- and microvascular endothelial dysfunction in

diabetes. J. Diabetes *9*, 434–449. https://doi.org/10.1111/1753-0407.12521.

34. Paulus, W.J., and Tschöpe, C. (2013). A novel paradigm for heart failure with preserved ejection fraction: comorbidities drive myocardial dysfunction and remodeling through coronary microvascular endothelial inflammation. J. Am. Coll. Cardiol. *62*, 263–271. https://doi.org/10.1016/j.jacc.2013.02.092.

35. Achari, A.E., and Jain, S.K. (2017). Adiponectin, a therapeutic target for obesity, diabetes, and endothelial dysfunction. Int. J. Mol. Sci. *18*, 1321. https://doi.org/10.3390/ijms18061321.

36. Almabrouk, T.A.M., White, A.D., Ugusman, A.B., Skiba, D.S., Katwan, O.J., Alganga, H., Guzik, T.J., Touyz, R.M., Salt, I.P., and Kennedy, S. (2018). High fat diet attenuates the anticontractile activity of aortic PVAT via a mechanism involving AMPK and reduced adiponectin secretion. Front. Physiol. *9*, 51. https://doi.org/10.3389/fphys.2018.00051.

37. Diggins, N.L., and Webb, D.J. (2017). APPL1 is a multifunctional endosomal signaling adaptor protein. Biochem. Soc. Trans. *45*, 771–779. https://doi.org/10.1042/bst20160191.

38. Fang, H., and Judd, R.L. (2018). Adiponectin regulation and function. Compr. Physiol. *8*, 1031–1063. https://doi.org/10.1002/cphy.c170046.

39. Nader, N., Dib, M., Hodeify, R., Courjaret, R., Elmi, A., Hammad, A.S., Dey, R., Huang, X.Y., and Machaca, K. (2020). Membrane progesterone receptor induces meiosis in Xenopus oocytes through endocytosis into signaling endosomes and interaction with APPL1 and Akt2. PLoS Biol. *18*, e3000901. https://doi.org/10.1371/journal.pbio.3000901.

40. Mao, X., Kikani, C.K., Riojas, R.A., Langlais, P., Wang, L., Ramos, F.J., Fang, Q., Christ-Roberts, C.Y., Hong, J.Y., Kim, R.Y., et al. (2006). APPL1 binds to adiponectin receptors and mediates adiponectin signalling and function. Nat. Cell Biol. *8*, 516–523. https://doi.org/10.1038/ncb1404.

41. Cheng, K.K.Y., Lam, K.S.L., Wang, Y., Huang, Y., Carling, D., Wu, D., Wong, C., and Xu, A. (2007). Adiponectin-induced endothelial nitric oxide synthase activation and nitric oxide production are mediated by APPL1 in endothelial cells. Diabetes *56*, 1387–1394. https://doi.org/10.2337/db06-1580.

42. Huang, P., Yan, R., Zhang, X., Wang, L., Ke, X., and Qu, Y. (2019). Activating Wnt/β-catenin signaling pathway for disease therapy: challenges and opportunities. Pharmacol. Ther. *196*, 79–90. https://doi.org/10.1016/j.pharmthera.2018.11.008.

43. Yin, P., Wang, W., Zhang, Z., Bai, Y., Gao, J., and Zhao, C. (2018). Wnt signaling in human and mouse breast cancer: focusing on Wnt ligands, receptors and antagonists. Cancer Sci. *109*, 3368–3375. https://doi.org/10.1111/cas.13771.

44. Chen, S., Zhang, M., Li, J., Huang, J., Zhou, S., Hou, X., Ye, H., Liu, X., Xiang, S., Shen, W., et al. (2022). β-catenin-controlled tubular cell-derived exosomes play a key role in fibroblast activation via the OPN-CD44 axis. J. Extracell. Vesicles *11*, e12203. https://doi.org/10.1002/jev2.12203.

STAR★METHODS

KEY RESOURCES TABLE

REAGENT or RESOURCE	SOURCE	IDENTIFIER
Antibodies		
Rabbit monoclonal anti-reptin	Cell Signaling Technology	Cat#12668S; RRID: AB_2797987
Rabbit monoclonal anti-IgG	Cell Signaling Technology	Cat#14708S; RRID: AB_2798581
Rabbit monoclonal anti-APPL1	Cell Signaling Technology	Cat#3858S; RRID: AB_2056989
Rabbit monoclonal anti-Histone 2A	Cell Signaling Technology	Cat#7631S; RRID: AB_10860771
Rabbit monoclonal anti-GAPDH	Cell Signaling Technology	Cat#5174S; RRID: AB_10622025
Rabbit monoclonal anti-β-catenin	Cell Signaling Technology	Cat#8480S; RRID: AB_11127855
Rabbit monoclonal anti-Non-β-catenin	Cell Signaling Technology	Cat#8814S; RRID: AB_11127203
NF-κB Pathway Antibody Sampler Kit	Cell Signaling Technology	Cat#9936T; RRID: AB_561197
Rabbit monoclonal anti-CD44	Cell Signaling Technology	Cat#37259S; RRID: AB_2750879
Rabbit monoclonal anti-ICAM-1	Cell Signaling Technology	Cat#67836S; RRID: AB_2799738
Biological samples		
Serum of Healthy control subjects and Diabetes patients	Anzhen Hospital, Capital Medical University, Beijing, China	https://anzhen.org/
Chemicals, peptides, and recombinant proteins		
Recombinant Human gAcrp30/Adipolean	Peprotech.inc	CAS:25-450-21
Recombinant CD44 protein	®Sangon Biotech	CAS:D622619
Critical commercial assays		
BCA Protein Array Kit	Thermo Fisher Scientific, Inc.	CAS:23227
Qproteome Cell Compartment Kit		CAS:37502
The Transcription Factor Activation Profiling Plate Array II	Signosis, Sunnyvale, CA	CAS: FA-1002
RT2 ProfilerTM PCR Array Human Transcription Factors	Qiagen, USA	GeneGlobe ID-PAHS-075ZA-24; CAS: 330231
ELISA Kit for Adiponectin (ADPN)	Cloud-Clone Corp	CAS: SEA605Hu
ELISA Kit for CD44	Cloud-Clone Corp	CAS: SEA670Hu
EZ-Link Sulfo-NHS-LC-Biotinylation kit	Thermo Fisher Scientific, Inc.	CAS:21435
Deposited data		
Raw and analyzed data	This paper	GEO: GSE217607
Experimental models: Cell lines		
Human umbilical vein endothelial cells (HUVECs): 4201HUM-CCTCC00635	NICR	http://cellresource.cn/fdetail.aspx?id=5307/
Experimental models: Organisms/strains		
Mouse: APPL1$^{-/-}$, 8 weeks's old	BRL Medicine Inc.	N/A
Mouse: APN$^{-/-}$, 8 weeks's old	Gift	N/A
Oligonucleotides		
siRNA targeting sequence: APPL1 #1: UCUCACCUGACUUCGAAACU	This paper	N/A
siRNA targeting sequence: CD44 #1: GAACAAGGAGUCGUCAGAAACUCCA	This paper	N/A
Primers, see Table S2	This paper	N/A

(*Continued on next page*)

Continued

REAGENT or RESOURCE	SOURCE	IDENTIFIER
Software and algorithms		
GraphPad Prism 8.0	GraphPad Software Inc., San Diego, CA	https://www.graphpad.com/
SPSS Statistics 25.0	SPSS Inc., Chicago, IL	https://www.ibm.com/

RESOURCE AVAILABILITY

Lead contact

Further information and requests for sources and reagents should be directed to and will be fulfilled by the corresponding author, Yunhui Du, PhD (annahhdu820@mail.ccmu.edu.cn).

Materials availability

The study did not generate new unique reagents. Primers and siRNA sequences used were provided in key resources table and Table S2, and available upon request to the corresponding author.

Data and code availability

- The high-throughput sequencing data reported in this paper have been submitted to GEO with accession number: GSE217607.
- This paper does not report original code.
- Any additional information required to reanalyze the data reported in this paper is available from the lead contact upon request.

EXPERIMENTAL MODEL AND SUBJECT DETAILS

Human subjects

74 type 2 diabetes patients (male vs. female: 48/26) and 35 healthy control subjects (male vs. female: 22/8) were recruited from Anzhen Hospital, Capital Medical University, Beijing, China. The clinical characteristics of diabetes patients are summarized in Table S1. The study protocol was approved by the Institutional Committee for the Protection of Human Subjects of Capital Medical University. All participants had written informed consent prior to enrollment. The protocol was approved by the Ethics Committee of Beijing Anzhen Hospital (No. 2017005) and complied with the Declaration of Helsinki. Both oral and written informed consents were obtained from all the participants. Venous blood samples were collected at admission without anticoagulant. After centrifugation at 4°C, the plasma was immediately separated and stored at −80 °C until further analysis. To avoid confounding data, we excluded patients with a history of stroke, type 1 diabetes mellitus (T1DM), valvular heart diseases, severe cardiovascular disease (CVD, cardiac function level at III or IV by New York Heart Association standards), severe hepatic and renal insufficiency, infectious diseases in the past two months, active liver diseases, hemodialysis, malignancy, pregnancy or hyperthyroidism.

Type 2 diabetic mice model

All experiments of this study were performed in adherence to the NIH Guidelines on the Use of Laboratory Animals and approved by the Research Ethics Committee of Capital Medical University (NO. AEEI-2020-112). APN knockout mice (male $APN^{-/-}$, 8 weeks's old, 20 ± 2g), APPL1 knockout mice (male $APPL1^{-/-}$, 8 weeks's old, 20 ± 2g), and C57BL/6 mice (male, 8 weeks's old, 20 ± 2g) were utilized in this study. WT mice were purchased from Beijing Si-Bei-Fu Experimental Animal Technology Co., Ltd. APPL1 knockout mice were purchased from BRL Medicine Inc. APN knockout mice were gifted by Yanqing Zhang Professor, the first affiliated hospital of Shanxi Medical Unverisy. The mice were randomized to feed a high-fat diet (HFD) (60% kcal fat, D12492i; Research Diets Inc.) or a standard diet control (ND, D12450Bi) for 12 weeks to induce 2 type diabetes, determined by fast blood glucose (Figure S1A). After 12 weeks, mice were either received vehicle or globular adiponectin treatment (0.25 μg/g/day intraperitoneal), determined by serum APN (Figure S1B), or CD44 C-terminal polypeptides treatment (0.25 μg/g/day intraperitoneal) via miniosmotic pump, ALZET, DURECT Corp, Cupertino, CA) for two extra weeks.

Cell lines

Human umbilical vein endothelial cells (HUVECs) were purchased from Cellbiologics Company (Cat NO. H-6207). HUVECs were either received the normal glucose/normal lipid or the high glucose (4.5 g/L)/ high lipids (HGHL) containing 25 mM d-glucose and 250 μM palmitates in Endothelial cell medium after reaching 80% confluence at 37°C in a humidified atmosphere of 5% CO2. Both culture media contain 10% fetal bovine serum (FBS) and endothelial cell growth factors according to the manufacturer's instructions.

METHOD DETAILS

Co-immunoprecipitation and western blot analysis

Cells were washed once with PBS, and lysed with cold 1×lysis buffer supplemented with a protease inhibitor cocktail I (Thermo Fisher Scientific, 78438).The cell lysate by adding 1.0 μg of the appropriate control IgG, together with 20 μL of resuspended volume of Protein A/G Plus-Agarose. Incubate at 4°C for 30 min. Cleared lysate was then incubated with normal immunoglobulin G (IgG) and anti-reptin (Cell Signaling Technology, #12668)) primary antibodies together with 15 μL pre-washed Protein A beads at 4 °C overnight. The immunoprecipitated proteins were released from the beads using an elution buffer. Samples were boiled and analyzed by Western blot.

Mouse aortic vascular tissues and cells were harvested and lysed to get total protein. Protein concentrations were determined by BCA Protein Array Kit (Thermo Fisher Scientific, Inc. 23227). Total proteins were separated by gel electrophoresis, and transferred to a polyvinylidene fluoride membrane. The membranes were blocked in 5% nonfat milk for 1h, and subsequently probed overnight at 4°C with primary antibodies, followed by secondary HRP-conjugated antibody at RT for 1h, and subsequently detected the protein bands by BioRad Imaging System. Antibodies against APPL1 (#3858), Histone 2A (#7631), GAPDH (#5174), β-catenin(#8480), Non-phospho (Active) β-catenin(#8814), Phospho-β-catenin(#9561), Reptin(#12668) were from Cell Signaling Technology (Beverly, MA).

Small interfering RNA transfection

RNA oligonucleotides complementary to Occludin, APPL1 target sequences silenced respective gene expression. Human umbilical vein endothelial cells were transfected with a Lipofectamine 3000 Transfection Kit(Thermo Fisher Scientific, Inc) per manufacturer's protocol with siRNA duplexes against APPL1(5′-UCUCACCUGACUUCGAAACUdTdT-3″3′), CD44(5′-GAACAAGGAGUCGUCAGAAAC UCCA-3″3′), and universal control oligonucleotides (AllStars, Westerville, OH). Briefly, cells were plated on six-well plates before transfection. After reaching 80% confluence, siRNA was applied to each well (final concentration 50 nM).

Cell compartment isolation

Cell fraction proteins were extracted by using the Qproteome Cell Compartment Kit per manufacturer's instructions (Qiagen, Cat No: 37502). Briefly, cells were washed by ice-cold PBS, harvested from the plate, and centrifuged (500g, 10 min at 4°C). The supernatant was discarded, and the cell pellet was resuspended by utilizing Extraction Lysis Buffer and incubated for 10 min at 4°C. After 10 min of centrifugation (1000 g at 4°C), the supernatant primarily contains cytosolic proteins. The cell pellet was resuspended by utilizing 7 μL Benzonase Nuclease and 13 μL distilled water. After 15 min of incubation (room temperature), nuclear lysis buffer was added to the cell extracts (10 min at 4°C), and then centrifugated for 10 min (6800g, 4°C). The supernatant mainly contains the nuclear fraction.

Transcription factor (TF) profiling array

The Transcription Factor Activation Profiling Plate Array II (Signosis, Sunnyvale, CA) was used to analyze the activity of transcription factors in HUVEC cells according to manufacturer's instructions. Nuclear proteins from HUVEC cells were isolated using a Nuclear Extraction Kit (Signosis, Sunnyvale, CA). Biotin labeled probes based on the consensus sequences of transcription factor DNA-binding sites were mixed with 15 μg of nuclear protein extract to form transcription factor/probe complexes. The bound probes were separated from the complex and hybridized to a plate that was pre-coated with sequences complementary to the probes. The captured DNA probe was detected with streptavidin-HRP, and signal intensity was measured with a microplate luminometer. Relative gene expression levels were calculated using the $\Delta\Delta C_T$ method with normalization to the average expression level of five housekeeping genes.

RNA sequencing

The total RNA was isolated from mouse aortic tissue by TRIzol method (Invitrogen). The mRNA was reverse transcribed into double-strand cDNA fragments. The mRNA Library was generated by NEB Next Ultra Directional RNA Library Prep Kit for Illumina (#E7530L, NEB, Ispawich, USA) according to the manufacturer's protocol. Final library quality control was performed, and RNA libraries were then sequenced at 10p.m. on the Illumina HiSeq 4000 to generate 150-bp pair-end reads. Differential expression analysis for RNA-seq was performed by DESeq2 v1.20.0 (http://bioconductor.org/packages/release/bioc/html/DESeq2.html).

Bioinformatics analysis

Functional annotation was conducted by GO enrichment analysis (Gene Ontology, http://geneontology.org/) to determine the genes that are significantly altered. Pathway analysis, predominantly based on the Kyoto Encyclopedia of Genes and Genomes (KEGG) database, was employed to determine the significant functions and pathways of DEGs. Only pathway categories with an FDR-corrected p value less than 0.05 were chosen. A hypergeometric p value is calculated and adjusted as FDR, where the background is set to be genes in the whole genome. GO terms with FDR.

RT^2 Profiler PCR array human transcription factors and quantitative Real-Time PCR (qRT-PCR) analysis

The Human Transcription Factors (Qiagen, USA) was used to analyze the mRNA level of Wnt/β-catenin pathway transcription factors in HUVEC cells according to manufacturer's instructions. Total RNA was isolated by Trizol reagent method (Invitrogen). Total RNA was used for first-strand cDNA synthesis. qRT-PCR was performed utilizing RT^2 SYBR Green Mastermix (PARN-026Z, QIAGEN) on the 7500 Real-Time PCR system (Thermo Fisher Scientific, Inc). PCR conditions included initial denaturation at 95°C for 10 min, 95°C for 15 s for 40 cycles, and 60°C for 1 min. Gene expression levels were calculated using the CT value. And fold-changes in expression were determined with the $2^{-\Delta\Delta CT}$. All samples were run in triplicate. For qPCR, primers were purchased from Sangon Biotech (Table S2).

Enzyme-linked immunosorbent assay (ELISA)

At inclusion, blood samples were taken for investigation of Adiponectin and CD44. Serum samples were collected at enrollment and immediately stored at −80°C in a single biologic resource center. Serum Adiponectin and CD44 levels were determined by commercial ELISA kit (Cat #8B5D6EB29B,Cat#38E7963A34, Cloud-Clone Corp) per manufacturer's instructions. The detection threshold was 0.156 and 1.56 ng/mL. Samples, reagents, and buffers were prepared according to the manufacturer's instructions.

BLI binding array

Real-time binding assays between Reptin and β-catenin/APPL1 were performed using BLI with an Octet Red 96 instrument (Fortebio). In the BLI experiments, Reptin protein was biotinylated by the EZ-Link Sulfo-NHS-LC-Biotinylation kit (catalog No. 21435) from Thermo Scientific. Briefly, we incubated Reptin protein and Sulfo-NHS-LC-biotin at 1:1 M ratio in double-distilled H_2O (600 μL volume), at 25°C for 30 min. After that, the excess free Sulfo-NHS-LC-biotin was removed by applying the protein sample to a desalting column (Zeba Spin Desalting Columns, 5 mL, for 500-2000 μL samples, 7000 molecular weight cutoff). After centrifugation of the column at 1000 g for 2 min, the collected flow-through solution is the biotin-labeled Reptin protein for subsequent BLI experiments.

Biotinylated Reptin was first immobilized onto streptavidin biosensors (ForteBio) at a speed of 111g for 4 min. The immobilized sensors were equilibrated in reaction buffer at a speed of 4.44g for 3 min. To analyze the effect of the global Adiponectin on the interaction between Reptin and APPL1 or β-catenin, a solution of 1 μg/μl of adiponectin was used for treating 1 μg/μl β-catenin or APPL1 in 30 μL kinase buffer at 37°Cfor 30 min. Association curves were obtained by incubating a Reptin-coated biosensor with different concentrations of APPL1 or β-catenin solutions with global Adiponectin treatment or without. At the same time, the dissociations also were detected by incubating in reaction buffer without APPL1 or β-catenin proteins in the same condition. Data were acquired using an Octet Data Acquisition 7.0.1.17, according to the 'manufacturers' instructions. The assays were analyzed with the Octet Data Analysis Software 7.0.1.3.

Fluorescence resonance energy transfer (FRET) analysis

HUVECs were stained with CFP-labeled Reptin and YFP-labeled β-catenin and then visualized by confocal microscope. An acceptor bleaching protocol was employed to measure the FRET efficiency as described previously. The FRET efficiency was calculated through the following formula: Efret = 1-CFPpre/CFPpost).

CHIP-sequencing and peak finding

Input DNA and CHIP DNA were prepared for ChIP sequencing via Illumina kit per manufacturer's protocol. Briefly, each sample was subjected to end repair, followed by addition of an A base to the 3′ end. Adapter ligated DNA fragments were size-selected (175–225 bp), PCR-amplified, and further size-selected (175–225 bp). Amplification and size selection were confirmed by a BioAnalyzer. DNA fragments were pooled and sequenced on an Illumina HiSeq-1000 sequencer. CHIP sequencing data was obtained via Illumina Genome Analyzer II. 36 base pairs were analyzed by Illumina's pipeline software for quality filtering, and aligned to Human genome(HG19) using BOWTIE software (V2.2.7). Only uniquely aligned reads were kept for subsequent bioinformatics analysis. To identify TCF peaks, We analyzed the Chip-seq data by the latest version of MACS2 software. Statistically significant CHIP-enriched regions (peaks) were identified by comparsion of IP vs Input or comparision to a Poisson background model (cut-off p value = 10^{-4}). UCSC Refseq database was used to annotate the genomic location of identified peaks.

QUANTIFICATION AND STATISTICAL ANALYSIS

Normally distributed data are expressed as mean ± SEM. Comparisons were evaluated between two groups using a t-test. One-way ANOVA was performed followed by Bonferroni post hoc test for differences between more than two groups. Comparisons between each group were made by post hoc analysis via Tukey test. Non-normal data are presented as medians (with interquartile ranges). The Wilcoxon rank-sum test was used to compare between groups. Statistical analysis was performed using GraphPad Prism 8.0 (GraphPad Software Inc., San Diego, CA) and SPSS 25.0 (SPSS Inc., Chicago, IL) software.